High-Sensitivity Metamaterial-Inspired Sensor for Microfluidic Dielectric Characterization

Amir Ebrahimi, *Student Member, IEEE*, Withawat Withayachumnankul,
Said Al-Sarawi, *Member, IEEE*, and Derek Abbott, *Fellow, IEEE*

Abstract—A new metamaterial-inspired microwave microfluidic sensor is proposed in this paper. The main part of the device is a microstrip coupled complementary split-ring resonator (CSRR). At resonance, a strong electric field will be established along the sides of CSRR producing a very sensitive area to a change in the nearby dielectric material. A micro-channel is positioned over this area for microfluidic sensing. The liquid sample flowing inside the channel modifies the resonance frequency and peak attenuation of the CSRR resonance. The dielectric properties of the liquid sample can be estimated by establishing an empirical relation between the resonance characteristics and the sample complex permittivity. The designed microfluidic sensor requires a very small amount of sample for testing since the cross-sectional area of the sensing channel is over five orders of magnitude smaller than the square of the wavelength. The proposed microfluidic sensing concept is compatible with lab-on-a-chip platforms owing to its compactness.

Index Terms—Complementary split-ring resonator (CSRR), dielectric characterization, metamaterial, microfluidic sensor.

I. Introduction

MICROWAVE sensors are very attractive choices for many of electronic, biomedical and industrial applications [1], [2]. They offer many advantages including high sensitivity, robustness and low fabrication and measurement costs [3]. These advantages make them preferable choices for microfluidic and biosensing applications [4], [5]. High sensitivity and accurate identification of chemical and biological liquid samples using microwave dielectric and cylindrical resonators have been studied and demonstrated [5]–[9]. In these applications, the resonance frequency changes and the transmission characteristics at resonance are used for determination of the complex permittivity. Notably, a relatively large device size makes these type of sensors unsuitable for integrated systems. In [10], a compact microwave sensor is designed for broadband microfluidic permittivity measurement

with complicated mathematical post-processing. In [11], a new K-band microfluidic device was proposed based on a quarter-wavelength resonator designed on coplanar waveguide. It employs a change in the resonance frequency for dielectric characterization. Despite the compactness and high sensitivity, the quality factor of the resonance is moderate, affecting the measurment accuracy for a small change in the dielectric properties.

Recently, a new microwave sensing platform is being developed using the concept of metamaterials [12], [13]. Metamaterials are artificially engineered materials made of sub-wavelength resonators that can manipulate the electromagnetic waves in a way causing some exotic electromagnetic properties [14]. Metamaterial inspired devices are suited to sensing applications since they offer improved compactness and a high Q-factor that is very sensitive to environmental changes [15]. Various types of new or improved microwave and terahetz sensors have been introduced so far using this new concept for different sensing applications such as displacement [16]–[18], rotation [17], [19] thin-film sensing [20]–[22], and strain sensing [23], [24]. Further to that, there are a few studies on metamaterial-based microfluidic characterization. In [25] and [26] microfluidic channels were designed to deliver the fluid sample to an array of resonators causing a significant modification of the resonance frequency. Nevertheless, this configuration requires a large amount of liquid sample for identification. In addition, a left handed planar medium formed, by using a spiral-resonator coupled microstrip line was designed together with a microfluidic channel for liquid sensing [27]. This device shows a bandpass response that is not accurate for dielectric characterization. Recently, we proposed a metamaterial-based microfluidic sensor with a single split-ring resonator (SRR) coupled microstrip line [28]. The microfluidic channel was considered in the gap area of the SRR where there is a very strong and localized electric field on resonance. Applying the liquid sample to this capacitive gap modifies the resonance frequency and quality factor from which the complex permittivity of mixtures can be determined. However, the sensitivity of the device was not enough to discriminate small changes in the permittivity of the sample as the maximum resonance frequency shift was reported to be around 100 MHz for a permittivity change of 80 [28].

In this paper, a complementary split-ring resonator (CSRR) is used instead of a SRR, to provide a larger area of fringing electric field that increases the effective interaction area with the sample. The proposed sensor determines the complex
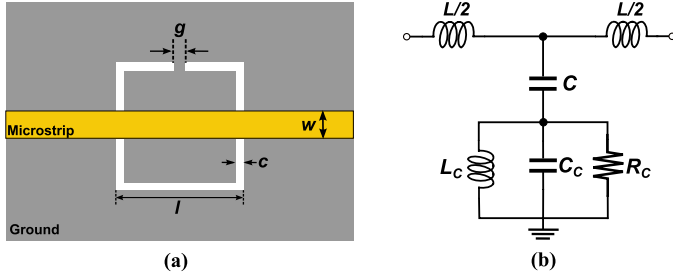
Fig. 1. (a) A microstrip coupled CSRR with the gray area showing the ground plane and yellow showing the top microstrip metalization. (b) Its equivalent circuit model with L and C for the unit length inductance and capacitance of the microstrip respectively and $\{RLC\}_C$ for the CSRR. The CSRR and microstrip dimensions are: $w = 1.3$ mm, $l = 11$ mm, $c = 0.5$ mm and $g = 0.2$ mm.

Fig. 2. Simulated resonance of the microstrip coupled CSRR of Fig. 1 in CST microwave studio. The resonance appears as a transmission zero in S_{21} around 2.4 GHz. A strong electric field is established between the capacitive plate and the ground plane at resonance.

permittivity of liquids based on changes in the resonance frequency and peak attenuation of the transmission response ($|S_{21}|_{\max}$) on resonance. The device is designed to operate at around 2 GHz and is compatible with lab-on-a-chip. So, it satisfies the need for low-cost and compact high sensitivity devices in microwave microfluidic applications.

The next section describes the sensing concept and the operation principle of the sensor. The fabrication process and measurement setup are explained in Section III. A sensing model is developed for the designed device in Section IV. The proposed microfluidic sensing method is validated through measurements in Section V and finally, Section VI forms the conclusion.

II. OPERATION PRINCIPLE

The main part of the proposed sensor structure is a microstrip coupled CSRR as shown in Fig. 1(a). The CSRR is composed of a metallic capacitive plate that is connected through an inductive metallic path to the surrounding ground plane at a distance c from its edge. Since the CSRR is etched in ground plane and is mainly excited by the electric field of the microstrip line, the whole coupled structure can be modelled by the lumped element circuit in Fig. 1(b) [29]. In the equivalent circuit model, the parallel combination of L_C, C_C and R_C models the CSRR, where C_C stands for the capacitor between the square-shaped metallic plate and the ground plane, L_C stands for the inductance of the metallic inductive path of width g connecting the capacitive plate to ground, and R_C models the equivalent loss associated with the CSRR [30]. Here, L and C model the inductance and capacitance of the microstrip line, respectively.

When the microstrip is fed with a microwave signal, it develops a quasi-TEM electromagnetic wave propagation mode described by a magnetic field circulating around the microstrip and an electric field pointing towards the ground plane. This electric field excites the CSRR inducing a voltage difference between the capacitive plate and the ground plane. The resonance occurs when the electric energy stored in the C and C_C capcitors equals to magnetic energy of the inductive strip of L_C. As shown in Fig. 2, at resonance, a strong electric field will be established across the gap between the capacitive plate and ground. The electric field is stronger across the
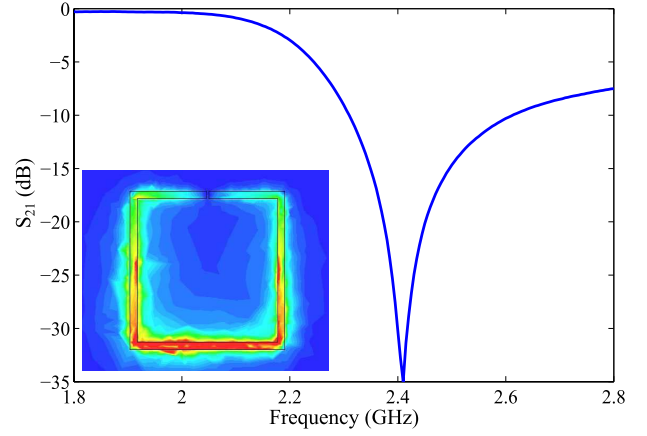
lower edge of the square-shaped CSRR making this region very sensitive to dielectric changes. Therefore, a microfliuidic channel is laid across the lower edge of the CSRR. The resonance can be observed as a notch in the transmission coefficient of the structure as illustrated in Fig. 2. From the circuit model of Fig. 1(b), the resonance frequency can be defined as [30]

$$f_0 = \frac{1}{2\pi \sqrt{L_C(C + C_C)}}, \qquad (1)$$

and the quality factor of the resonance is

$$Q = R\sqrt{\frac{C + C_C}{L_C}}. \qquad (2)$$

It is worth noting that the capacitor C_C is affected by the dielectric materials near the gap between the CSRR and ground. So, it can be approximated by

$$C_C = C_0 + \epsilon_{\text{sam}} C_e, \qquad (3)$$

where, C_0 models the capacitive effects of the dielectric substrate, channel walls and surrounding space excluding the channel cavity and the term $\epsilon_{\text{sam}} C_e$ denotes the capacitive effect of the liquid sample loaded into the microfluidic channel. Here, C_e is the capacitance of the empty channel. Now, if the complex permittivity of the liquid sample is considered to be $\epsilon_{\text{sam}} = \epsilon'_{\text{sam}} + j\epsilon''_{\text{sam}}$, from (1)–(3), both of the resonance frequency and the quality factor will be functions of the liquid sample permittivity or

$$f_0 = F_1(\epsilon'_{\text{sam}}, \epsilon''_{\text{sam}}), \ Q = F_2(\epsilon'_{\text{sam}}, \epsilon''_{\text{sam}}). \qquad (4)$$

The above discussion indicates that the resonant characteristics of the microstrip coupled CSRR device are dominated by the complex permittivity of a liquid sample. Therefore, by analyzing this dependency, we can determine the complex permittivity of an unknown liquid sample simply by measuring the transmission resonance characteristics.
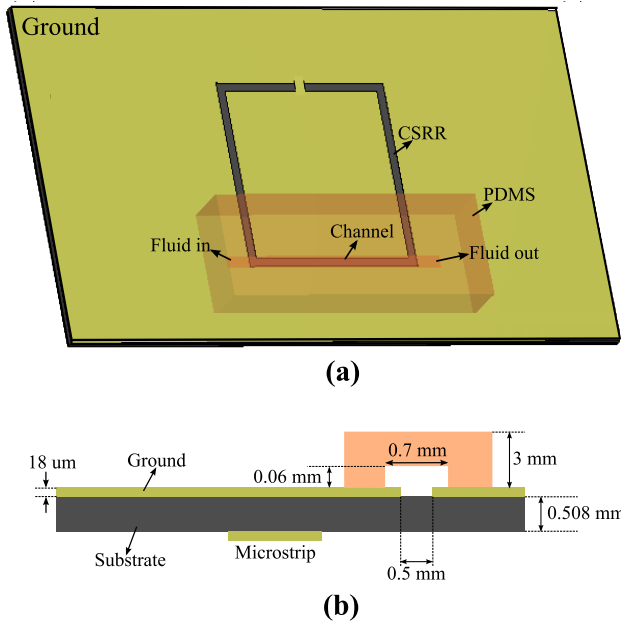
Fig. 3. Schematic of the microstrip coupled CSRR with the PDMS microfluidic channel (a) Top view of the structure (b) Side view with dimensions.

III. FABRICATION PROCESS

The designed device has been fabricated on Rogers RO6002 microwave substrate with a relative permittivity of 2.94 for allowing significant fringing field in the sensing area and hence increasing the sensitivity. The substrate thickness is 0.508 mm. The copper metalization for the ground plane and 50 Ω microstrip line is 18 μm.

As mentioned before, the microfluidic channel is positioned along the lower edge of the CSRR. The material used for channel is polydimethylsiloxane (PDMS) since it is inexpensive, widely available, biocompatible, durable, and easy to process [10], [11]. For channel fabrication, a mold has been prepared on a silicon substrate by using a thick photoresist mask and chemical etching. Then, a PDMS layer is deposited on the prepared mold and cured at 80 °C. Finally, the PDMS channel is peeled off and attached to the microstrip coupled CSRR. The channel is manually positioned to the lower side of CSRR where the fringing electric field is strongest and therefore, the sensitivity to the dielectric property changes is maximum. The height, width and length of the channel are 0.06 mm, 0.7 mm and 14 mm, respectively. Fig. 3 shows the bottom view and cross section of the structure when the channel is attached to the substrate.

The PDMS channel ensures a constant volume and shape of the liquid sample across the sensing area. It should be mentioned that the device response might be influenced by the position of the channel but it should not be an issue since the channel position is kept unchanged during all measurements. In a similar manner to [28], the measurements are carried out based on a stop-flow technique. A binary solution of distilled water and ethanol is used as a liquid sample for testing since it provides a broad range of the complex permittivity at the low microwave frequency range [31]. Teflon tubes, together with
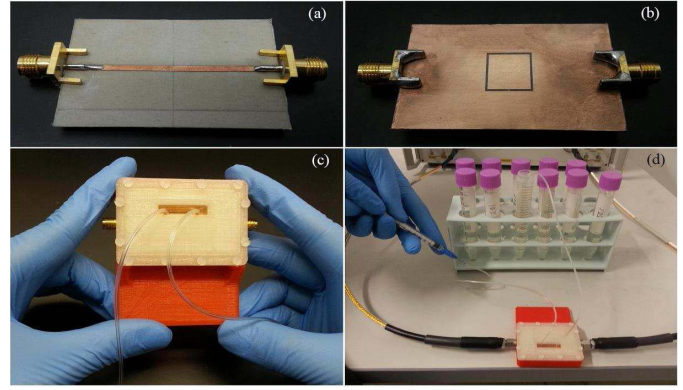

Fig. 4. The sensor module. (a) Top view of bare CSRR. (b) Bottom view of bare CSRR. (c) The complete sensor module when the PDMS channel and in/outlet tubes are attached and the device is packaged. (d) The complete test setup when the device is connected to the network analyzer for measurments.
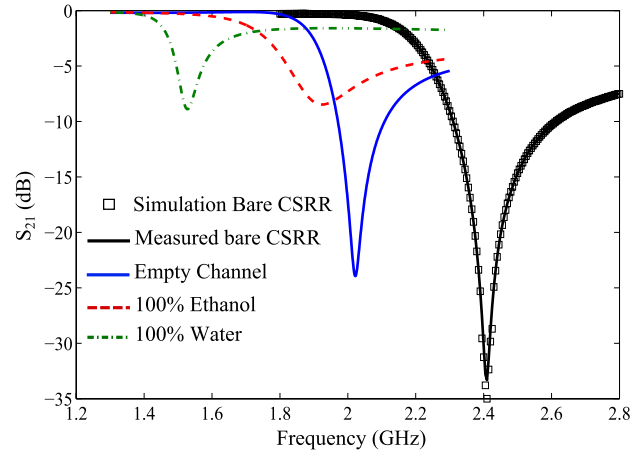

Fig. 5. Measured transmission response of the sensor in different conditions.

a syringe, connected to the inlet and outlet of the channel are used for filling and draining the channel. The fabricated and assembled sensor is shown in Fig. 4 together with the measurement setup. During the measurements, a very low pressure is applied to the syringe to avoid channel deformation. In each step, the channel is firstly filled with the liquid sample and then the flow is stopped for measurement. The resonance frequency and peak attenuation parameters are then recorded to characterize the liquid test samples. As seen in Fig. 5, the resonance frequency and peak attenuation are maximum when the channel is not attached to the sensor. By adding the PDMS channel, the resonance frequency is shifted down with a small decrease of peak attenuation since a part of the CSRR is covered with the PDMS.

IV. DEVICE CHARACTERISTICS

A. Initial Measurements

For investigating the effect of the complex permittivity ($\epsilon'_{sam} + j\epsilon''_{sam}$) on the resonance frequency and peak attenuation, a set of experiments has been performed using binary mixtures of distilled water and ethanol. The dielectric properties of water-ethanol mixture was accurately studied in [31]. The accurate complex permittivity of the test fluid samples

TABLE I

COMPLEX PERMITTIVITY OF WATER-ETAHNOL MIXTURE AT 1.9 GHz
[28], [31]. THE VOLUME FRACTION OF WATER IS CHANGED
FROM 10% TO 90% FOR DEVICE TESTING

Water Fraction%	ϵ'	ϵ''	$\Delta\epsilon'$	$\Delta\epsilon''$
10	16.5	12.3	-30.5	-2.7
30	31.5	15.55	-15.5	0.55
50	47	15	0	0
70	61	12.8	14	-2.2
90	72	10.6	25	-4.4

from [28], [31] are listed in Table I. For the first set of measurements, the volume fraction of water is changed from 10% to 90% with a step size of 20% and at each step, the resonance frequency and peak attenuation of the sensor are recorded giving a data set of 5 samples. The measurement results of the resonance frequency and maximum attenuation for the 5 test samples are shown in Fig. 6. As seen, the resonance frequency is shifted from 1.875 GHz down to 1.57 GHz as the water volume fraction increases from 10% to 90%. The peak attenuation is minimum when the water volume fraction is 30%. It is worth noting that the observed nonlinearity in the peak attenuation with respect to the water content follows the nonlinear loss function of water mixture [28], [31].

B. Mathematical Model Derived from Measurments

Based on the measurement results of the five test samples, a simple model is derived for resonance frequency shift and peak attenuation variations as a function of the complex permittivity. This simplified model can be defined as

$$\begin{bmatrix} \Delta f_0 \\ \Delta|S_{21}| \end{bmatrix} = \begin{bmatrix} m_{11} & m_{12} \\ m_{21} & m_{22} \end{bmatrix} \begin{bmatrix} \Delta\epsilon'_{\text{sam}} \\ \Delta\epsilon''_{\text{sam}} \end{bmatrix}, \quad (5)$$

where, $\Delta\epsilon'_{\text{sam}} = \epsilon'_{\text{sam}} - \epsilon'_{\text{ref}}$, $\Delta\epsilon''_{\text{sam}} = \epsilon''_{\text{sam}} - \epsilon''_{\text{ref}}$ and $\Delta f_0 = f_{0\text{sam}} - f_{0\text{ref}}$ with subscript (sam) for the sample under test and (ref) for the reference mixture. Here, the mixture with a 50% water fraction is considered as the reference. The unknown parameters of the matrix can be determined from the data available from the measurement results of Fig. 6, together with the reported complex permittivity in Table 1. The benefit of this model is that all the fabrication tolerances of the device are fully taken into account. The coefficients of the model in (5) are over determined by test datasets. So, the least-squares method explained in [28] can be used to approximate the coefficients. This method yields the following matrix that relates the resonance frequency and maximum attenuation changes to the complex permittivity

$$\begin{bmatrix} \Delta f_0 \\ \Delta|S_{21}| \end{bmatrix} = \begin{bmatrix} -0.00528 & 0.000256 \\ -0.00045 & -0.292 \end{bmatrix} \begin{bmatrix} \Delta\epsilon'_{\text{sam}} \\ \Delta\epsilon''_{\text{sam}} \end{bmatrix}. \quad (6)$$

By comparing the coefficients in (6), it will be found that the effect of ϵ' on the resonance frequency is approximately 20 times larger than the effect of ϵ''. On the other hand, the impact of ϵ'' on the peak attenuation is 650 times higher than the influence of ϵ'.
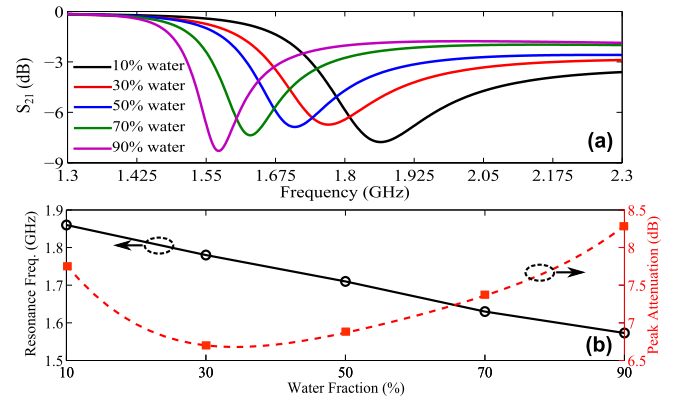

Fig. 6. (a) The measured transmission response of the water-ethanol test samples for calibration of the sensor. The water volume fraction is changed from 10% to 90% with the step size of 20%. (b) Corresponding resonance frequency and peak attenuation at different steps with dashed line for visual guidance.

TABLE II

COMPLEX PERMITTIVITY OF WATER-ETAHNOL MIXTURE AT 1.9 GHz
[28], [31]. THE VOLUME FRACTION OF WATER IS
CHANGED FROM 0% TO 100%

Water Fraction%	ϵ'	ϵ''	$\Delta\epsilon'$	$\Delta\epsilon''$
0	9	10	-38	-5
20	24	13.6	-23	-1.4
40	39	15.6	-8	0.6
60	53	14.6	6	-0.4
80	67	13.4	20	-1.6
100	79.5	9	32.5	-6

Considering the samples of Table I

$$\left|\frac{\Delta\epsilon'}{\Delta\epsilon''}\right|_{\text{max}} \approx 28, \qquad \left|\frac{\Delta\epsilon''}{\Delta\epsilon'}\right|_{\text{max}} \approx 0.176. \quad (7)$$

So, by neglecting m_{12} and m_{21} the maximum errors of Δf_0 is

$$\left|\frac{m_{12}\Delta\epsilon''}{m_{11}\Delta\epsilon'}\right|_{\text{max}} \approx 0.9\%, \quad (8)$$

and the maximum error in $\Delta|S_{21}|$ can be obtained as

$$\left|\frac{m_{21}\Delta\epsilon'}{m_{22}\Delta\epsilon''}\right|_{\text{max}} \approx 4.3\%. \quad (9)$$

From (8) and (9) it can be inferred that the contributions of ϵ'' on the resonance frequency shift and ϵ' on the peak attenuation changes are negligible. So, the characteristic matrix of (6) can be simplified as

$$\begin{bmatrix} \Delta f_0 \\ \Delta|S_{21}| \end{bmatrix} = \begin{bmatrix} -0.00528 & 0 \\ 0 & -0.292 \end{bmatrix} \begin{bmatrix} \Delta\epsilon'_{\text{sam}} \\ \Delta\epsilon''_{\text{sam}} \end{bmatrix}. \quad (10)$$

The complex permittivity of unknown liquid samples can be determined using matrix inversion. Inverting (10) leads to

$$\begin{bmatrix} \Delta\epsilon'_{\text{sam}} \\ \Delta\epsilon''_{\text{sam}} \end{bmatrix} = \begin{bmatrix} -189.39 & 0 \\ 0 & -3.424 \end{bmatrix} \begin{bmatrix} \Delta f_0 \\ \Delta|S_{21}| \end{bmatrix}, \quad (11)$$

which can be used for determining the complex permittivity of unknown liquid samples simply just by measuring the resonance characteristics.
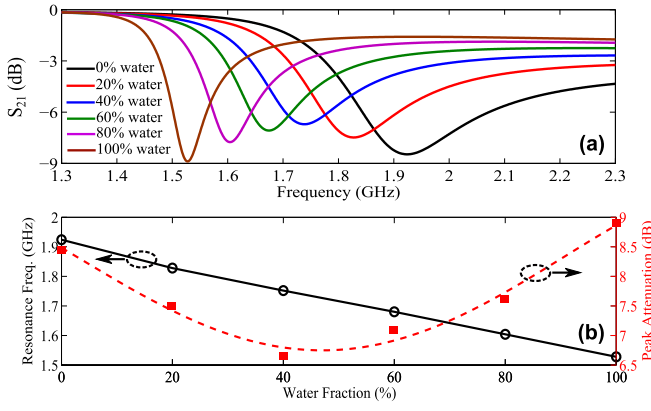
Fig. 7.   (a) The measured transmission response of the water-ethanol test samples for validating of the (11) model. The water volume fraction is changed from 20% to 100% with the step size of 20%. (b) Corresponding resonance frequency and peak attenuation at different steps with dashed line for visual guidance.
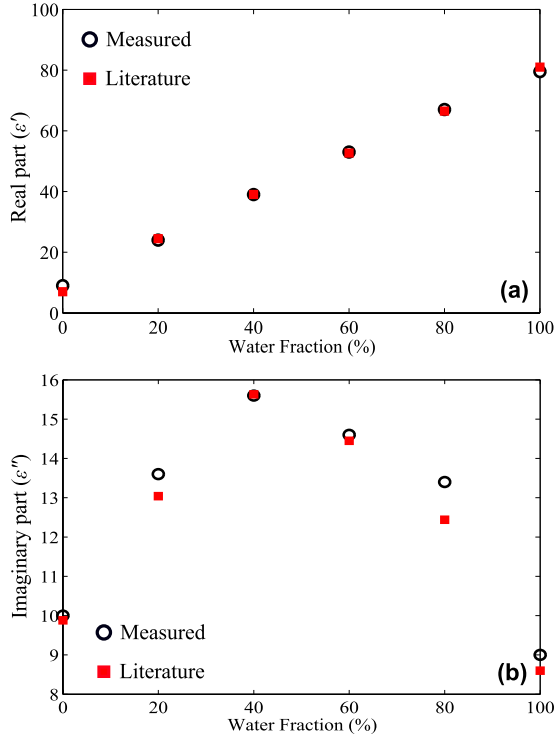

Fig. 8.   Comparison between the predicted and litrature values of complex permittivity for the water-ethanol mixture at around 1.9 GHz. The volume fraction of water is changed from 0% to 100% with the step size of 20%. (a) Real part of the complex permittivity. (b) Imaginary part of the complex permittivity.

V. EXPERIMENTAL RESULTS AND VALIDATION

In order to verify the presented sensor model in (11), the water ethanol mixture is used again. This time, the volume fraction of water is changed from 0% to 100% with the step size of 20% giving 6 data sets of measurement results. The measured transmission responses of the sensor for these sets of samples are shown in Fig. 7 together with the extracted resonance frequency and peak attenuation. As seen, the corresponding frequency shift for 0%–100% of the water volume fraction is around 400 MHz, showing 4 times higher sensitivity with respect to our previous design [28] with a

100 MHz frequency shift. The model presented in (11) is used to determine the $\Delta\epsilon'$ and $\Delta\epsilon''$ for each couples of measured resonance frequency and peak attenuation, where 50% water-ethanol mixture is considered as the reference. Then, the complex permittivity of each sample can be calculated as

$$\epsilon'_{\text{sam}} = \epsilon'_{\text{ref}} + \Delta\epsilon'_{\text{mod}} \qquad (12)$$

$$\epsilon''_{\text{sam}} = \epsilon''_{\text{ref}} + \Delta\epsilon''_{\text{mod}} \qquad (13)$$

with a subscript 'mod' for the values obtained from (11). For comparison, the obtained complex permittivity values of the samples are plotted against the exact values in Fig. 8. This figure shows an acceptable accuracy of the simplified model of (11). The small disagreements between the measured and literature values of complex permittivity may potentially arise from the measurement uncertainties or the simplified linear approximation of the sensing model. The accuracy can be increased by using a higher order approximation. The device can also be tested with other sets of liquid samples covering wider ranges of complex permittivity values to produce a more accurate sensing model.

VI. CONCLUSION

A simple and efficient concept for a microwave microfluidic sensor is proposed and validated. By exploiting the advantage of a microstrip-coupled CSRR, a very strong electric field is produced in a small area, resulting in a high sensitivity to the dielectric property of surrounding materials. A PDMS microfluidic channel has been attached along the lower edge of CSRR to deliver the fluidic sample to the sensing area where the cross section of the sensing channel is small as $2 \times 10^{-5}\lambda_0^2$. Binary mixtures of water-ethanol have been used to characterize the sensor. Measurement results show a good accuracy when using the proposed microfluidic sensor and the parameter estimation model. The proposed concept promises a high sensitivity and accurate microfluidic sensing at low microwave frequencies. Owing to its compact structure, the device has the potential to be integrated with system-on-a-chip.

REFERENCES

[1] A. Gregory and R. Clarke, "A review of RF and microwave techniques for dielectric measurements on polar liquids," *IEEE Trans. Dielectr. Electr. Insul.*, vol. 13, no. 4, pp. 727–743, Aug. 2006.

[2] M. Schueler, C. Mandel, M. Puentes, and R. Jakoby, "Metamaterial inspired microwave sensors," *IEEE Microw. Mag.*, vol. 13, no. 2, pp. 57–68, Mar./Apr. 2012.

[3] C. Mandel, B. Kubina, M. Schubler, and R. Jakoby, "Passive chipless wireless sensor for two-dimensional displacement measurement," in *Proc. 41st Eur. Microw. Conf.*, 2011, pp. 79–82.

[4] H.-J. Lee, J.-H. Lee, H.-S. Moon, I.-S. Jang, J.-S. Choi, J.-G. Yook, *et al.*, "A planar split-ring resonator-based microwave biosensor for label-free detection of biomolecules," *Sens. Actuators B, Chem.*, vol. 169, pp. 26–31, Jul. 2012.

[5] G. Gennarelli, S. Romeo, M. Scarfi, and F. Soldovieri, "A microwave resonant sensor for concentration measurements of liquid solutions," *IEEE Sensors J.*, vol. 13, no. 5, pp. 1857–1864, May 2013.

[6] K. Yu, S. G. Ogourtsov, V. G. Belenky, A. B. Maslenikov, and A. Omar, "Accurate microwave resonant method for complex permittivity measurements of liquids [biological]," *IEEE Trans. Microw. Theory Tech.*, vol. 48, no. 11, pp. 2159–2164, Nov. 2000.

[7] B. Kapilevich and B. Litvak, "Optimized microwave sensor for online concentration measurements of binary liquid mixtures," *IEEE Sensors J.*, vol. 11, no. 10, pp. 2611–2616, Oct. 2011.

[8] H. Kawabata and Y. Kobayashi, "Accurate measurements of complex permittivity of liquid based on a TM_{010} mode cylindrical cavity method," in *Proc. Eur. Microw. Conf.*, vol. 1. Oct. 2005, pp. 369–372.

[9] J. Kim, A. Babajanyan, A. Hovsepyan, K. Lee, and B. Friedman, "Microwave dielectric resonator biosensor for aqueous glucose solution," *Rev. Sci. Instrum.*, vol. 79, no. 8, pp. 086107-1–086107-3, 2008.

[10] K. Grenier, D. Dubuc, P.-E. Poleni, M. Kumemura, H. Toshiyoshi, T. Fujii, *et al.*, "Integrated broadband microwave and microfluidic sensor dedicated to bioengineering," *IEEE Trans. Microw. Theory Tech.*, vol. 57, no. 12, pp. 3246–3253, Dec. 2009.

[11] T. Chretiennot, D. Dubuc, and K. Grenier, "A microwave and microfluidic planar resonator for efficient and accurate complex permittivity characterization of aqueous solutions," *IEEE Trans. Microw. Theory Tech.*, vol. 61, no. 2, pp. 972–978, 2013.

[12] N. I. Zheludev, "The road ahead for metamaterials," *Science*, vol. 328, no. 5978, pp. 582–583, 2010.

[13] M. Huang and J. Yang, *Microwave Sensor Using Metamaterials*. Vienna, Austria: InTech, 2011, pp. 13–36.

[14] A. Ebrahimi, W. Withayachumnankul, S. Al-Sarawi, and D. Abbott, "Compact dual-mode wideband filter based on complementary split-ring resonator," *IEEE Microw. Wireless Compon. Lett.*, 2014, doi: 10.1109/LMWC.2013.2291869.

[15] T. Chen, S. Li, and H. Sun, "Metamaterials application in sensing," *Sensors*, vol. 12, no. 3, pp. 2742–2765, 2012.

[16] A. Horestani, C. Fumeaux, S. Al-Sarawi, and D. Abbott, "Displacement sensor based on diamond-shaped tapered split ring resonator," *IEEE Sensors J.*, vol. 13, no. 4, pp. 1153–1160, Apr. 2013.

[17] J. Naqui, M. Durán-Sindreu, and F. Martín, "Novel sensors based on the symmetry properties of split ring resonators (SRRs)," *Sensors*, vol. 11, no. 8, pp. 7545–7553, 2011.

[18] J. Naqui, M. Durán-Sindreu, and F. Martín, "Alignment and position sensors based on split ring resonators," *Sensors*, vol. 12, no. 9, pp. 11790–11797, 2012.

[19] A. Horestani, D. Abbott, and C. Fumeaux, "Rotation sensor based on horn-shaped split ring resonator," *IEEE Sensors J.*, vol. 13, no. 8, pp. 3014–3015, Aug. 2013.

[20] W. Withayachumnankul, H. Lin, K. Serita, C. M. Shah, S. Sriram, M. Bhaskaran, *et al.*, "Sub-diffraction thin-film sensing with planar terahertz metamaterials," *Opt. Exp.*, vol. 20, no. 3, pp. 3345–3352, 2011.

[21] W. Withayachumnankul, K. Jaruwongrungsee, C. Fumeaux, and D. Abbott, "Metamaterial-inspired multichannel thin-film sensor," *IEEE Sensors J.*, vol. 12, no. 5, pp. 1455–1458, May 2012.

[22] I. A. I. Al-Naib, C. Jansen, and M. Koch, "Thin-film sensing with planar asymmetric metamaterial resonators," *Appl. Phys. Lett.*, vol. 93, no. 8, pp. 083507-1–083507-3, 2008.

[23] R. Melik, E. Unal, N. K. Perkgoz, C. Puttlitz, and H. V. Demir, "Metamaterial-based wireless strain sensors," *Appl. Phys. Lett.*, vol. 95, no. 1, pp. 011106-1–011106-3, 2009.

[24] J. Li, C. M. Shah, W. Withayachumnankul, B. S.-Y. Ung, A. Mitchell, S. Sriram, *et al.*, "Flexible terahertz metamaterials for dual-axis strain sensing," *Opt. Lett.*, vol. 38, no. 12, pp. 2104–2106, Jun. 2013.

[25] B. Dong, W. Zhu, Y. H. Fu, J. Tsai, H. Cai, D. L. Kwong, *et al.*, "An absorptive filter using microfluidic switchable metamaterials," in *Proc. 16th Int. Solid-State Sensors, Actuat. Microsyst. Conf.*, 2011, pp. 530–533.

[26] J. A. Gordon, C. L. Holloway, J. Booth, S. Kim, Y. Wang, J. Baker-Jarvis, *et al.*, "Fluid interactions with metafilms/metasurfaces for tuning, sensing, and microwave-assisted chemical processes," *Phys. Rev. B*, vol. 83, pp. 205130-1–205130-5, May 2011.

[27] N. Wiwatcharagoses, K. Y. Park, J. Hejase, L. Williamson, and P. Chahal, "Microwave artificially structured periodic media microfluidic sensor," in *Proc. IEEE 61st ECTC*, May/Jun. 2011, pp. 1889–1893.

[28] W. Withayachumnankul, K. Jaruwongrungsee, A. Tuantranont, C. Fumeaux, and D. Abbott, "Metamaterial-based microfluidic sensor for dielectric characterization," *Sens. Actuators A, Phys.*, vol. 189, pp. 233–237, Jan. 2013.

[29] J. Baena, J. Bonache, F. Martín, R. Sillero, F. Falcone, T. Lopetegi, *et al.*, "Equivalent-circuit models for split-ring resonators and complementary split-ring resonators coupled to planar transmission lines," *IEEE Trans. Microw. Theory Tech.*, vol. 53, no. 4, pp. 1451–1461, Apr. 2005.

[30] J. Bonache, M. Gil, I. Gil, J. García-García, and F. Martín, "On the electrical characteristics of complementary metamaterial resonators," *IEEE Microw. Wireless Compon. Lett.*, vol. 16, no. 10, pp. 543–545, Oct. 2006.

[31] J.-Z. Bao, M. L. Swicord, and C. C. Davis, "Microwave dielectric characterization of binary mixtures of water, methanol, and ethanol," *J. Chem. Phys.*, vol. 104, no. 12, pp. 4441–4450, 1996.

Amir Ebrahimi (S'09) was born in Babol, Iran, on September 11, 1986. He received the B.Sc. degree in electrical engineering from the University of Mazandaran, Babol, in 2008, and the M.Sc. degree in electronic engineering from the Babol University of Technology, Babol. From 2009 to 2012, he was a Research Assistant with the Integrated Circuits Research Laboratory, Babol University of Technology. He is currently pursuing the Ph.D. degree in electrical and electronic engineering with the University of Adelaide, Australia. His research interests include metamaterial-inspired microwave devices, microwave circuit design, microwave filters, and frequency selective surfaces. Mr. Ebrahimi is a recipient of the International Postgraduate Research Ph.D. Scholarship, the Australian Postgraduate Award, and the Australian National Fabrication Facility Award for fabricating high performance microwave microfluidic sensors in collaboration with the Ian Wark Research Institute, University of South Australia.

Withawat Withayachumnankul received the B.Eng. (Hons.) and M.Eng. degrees in electronic engineering from the King Mongkut's Institute of Technology Ladkrabang, Thailand, in 2000 and 2002, respectively. From 2006 to 2008, he was an Australian Endeavour International Postgraduate Research Scholarship and University of Adelaide Scholarship for Postgraduate Research. He is currently pursuing the Ph.D. degree with the School of Electrical and Electronic Engineering, University of Adelaide. He received the IEEE/LEOS Graduate Student Fellowship and the SPIE Scholarship in Optical Science and Engineering. He is currently an ARC Post-Doctoral Research Fellow with the School of Electrical and Electronic Engineering, University of Adelaide, and an Associate Professor with RMIT University, Australia. His research interests include metamaterials, plasmonics, and terahertz spectroscopy.

Said Al-Sarawi (M'92) received the B.Eng. degree (1st Class Hons.) in marine radio communication and in marine electronics and communication from the Arab Academy for Science and Technology, Egypt, in 1987 and 1990, respectively, and the Ph.D. degree in mixed analog and digital circuit design techniques for smart wireless systems with special commendation in electrical and electronic engineering from The University of Adelaide, Australia, in 2003. He was awarded The University of Adelaide Alumni Postgraduate Medal (formerly Culross Prize) for outstanding academic merit at the postgraduate level. He received the Commonwealth Postgraduate Research Award (Industry). He received the Graduate Certificate in Education (Higher Education) with the same university in 2006. Currently, he is the Director of the Centre for Biomedical Engineering and a Founding Member of the Education Research Group of Adelaide, University of Adelaide. His research interests include design techniques for mixed signal systems in CMOS and optoelectronic technologies for high performance radio transceivers, low power and low voltage radio frequency identification systems, data converters, mixed signal design, and microelectromechanical systems for biomedical applications. His current educational research is focused on innovative teaching techniques for engineering education, research skill development, and factors affecting students evaluations of courses in different disciplines.

Derek Abbott (M'85–SM'99–F'05) was born in London, U.K., in 1960. He received the B.Sc. (Hons.) degree in physics from Loughborough University, U.K., in 1982, and the Ph.D. degree in electrical and electronic engineering from the University of Adelaide, Australia, in 1995, under K. Eshraghian and B. R. Davis. From 1978 to 1986, he was a Research Engineer with the GEC Hirst Research Centre, London. From 1986 to 1987, he was a VLSI Design Engineer with Austek Microsystems, Australia. Since 1987, he has been with the University of Adelaide, where he is currently a Full Professor with the School of Electrical and Electronic Engineering. He holds over 800 publications/patents and has been an invited speaker at over 100 institutions. He is a fellow of the Institute of Physics (IOP). He has received a number of awards, including the South Australian Tall Poppy Award for Science in 2004, the Premier's SA Great Award in Science and Technology for outstanding contributions to South Australia in 2004, and the Australian Research Council Future Fellowship in 2012. He has served as an Editor and/or Guest Editor for a number of journals, including the IEEE JOURNAL OF SOLID-STATE CIRCUITS, the *Journal of Optics B (IOP)*, *Microelectronics Journal (Elsevier)*, *Chaos (AIP)*, *Smart Structures and Materials (IOP)*, *Journal of Optics B (IOP)*, *Fluctuation Noise Letters (World Scientific)*, and is currently on the editorial boards of the PROCEEDINGS OF THE IEEE, the IEEE PHOTONICS JOURNAL, and *PLoS ONE*. He has co-edited *Quantum Aspects of Life, Imperial College Press*, co-authored *Stochastic Resonance* (Cambridge University Press) and *Terahertz Imaging for Biomedical Applications* (Springer-Verlag).

His interests are in the area of multidisciplinary physics and electronic engineering applied to complex systems. His research programs span a number of areas of stochastics, game theory, photonics, biomedical engineering, and computational neuroscience.